

## Original Article

## Positive Effects of Qing'e Pill (青娥丸) on Trabecular Microarchitecture and its Mechanical Properties in Osteopenic Ovariectomised Mice\*

SHUAI Bo, ZHU Rui, YANG Yan-ping, SHEN Lin, XU Xiao-juan, MA Chen, and LU Lin

**ABSTRACT** **Objective:** To investigate the impact of Qing'e Pill (青娥丸, QEP) on the cancellous bone microstructure and its effect on the level of  $\beta$ -catenin in a mouse model of postmenopausal osteoporosis. **Methods:** Ninety-six 8-week-old specific pathogen free C57BL/6 mice were randomly divided into 4 groups (24/group): sham, ovariectomised osteoporosis model, oestradiol-treated, and QEP-treated groups. Three months after surgery, the third lumbar vertebra and left femur of the animals were dissected and scanned using micro-computed tomography (micro-CT) to acquire three-dimensional (3D) parameters of their cancellous bone microstructure. The impact of ovariectomy, the effect of oestradiol and QEP intervention on cancellous bone microstructure, and the expression of  $\beta$ -catenin were evaluated. **Results:** The oestradiol- and the QEP-treated groups exhibited a significant increase in the bone volume fraction, trabecular number, trabecular thickness, bone surface to bone volume ratio (BS/BV), and  $\beta$ -catenin expression compared with those of the model group ( $P < 0.05$ ). In contrast, the structure model index, trabecular separation, and BS/BV were significantly decreased compared with those of the ovariectomised osteoporosis model group ( $P < 0.05$ ). No differences were observed in the above parameters between animals of the QEP- and oestradiol-treated groups. **Conclusions:** The increased  $\beta$ -catenin expression may be the mechanism underlying QEP's improvement of the cancellous bone microstructure in ovariectomised mice. Our findings provide a scientific rationale for using QEP as a dietary supplement to prevent bone loss in postmenopausal women.

**KEYWORDS** ovariectomised, osteoporosis, micro-Computed tomography, oestradiol, Qing'e Pill, Chinese medicine,  $\beta$ -catenin

Osteoporosis has often been evaluated by the measurement of bone mineral density (BMD). Various methods for BMD measurement have been developed, including X-ray, radiographic absorptiometry, single-photon absorptiometry, dual-photon absorptiometry, single-energy X-ray absorptiometry, and dual-energy X-ray absorptiometry (DEXA). Using BMD as an indicator for the evaluation and diagnosis of osteoporosis has profoundly contributed to the understanding of the pathogenesis, prevention, treatment, monitoring, and prognosis of osteoporosis. However, BMD measurement alone is insufficient because it is only a quantitative measurement of bone mineral and does not truly reflect the stability and the mechanical strength of cancellous bone.<sup>(1-4)</sup>

Pathological changes of osteoporosis occur mainly in cancellous bone. Cancellous bone is a structure of interconnected rods or plates that form a three-dimensional (3D) branching lattice. In osteoporosis, the amount of trabecular bone

is reduced and the bone becomes thinner, the intertrabecular space enlarges, the interconnected structure of trabecular bone is disrupted, trabecular perforation occurs in plate-like structures, or normal plate-like trabeculae are converted into thinner rod-like structures, which can even disappear, thereby increasing the risk of fracture. The assessment of microstructural changes of cancellous bone plays a significant role in the study of osteoporotic fracture and the evaluation of anti-osteoporotic agents. Micro-computed tomography (micro-CT), a high-

©The Chinese Journal of Integrated Traditional and Western Medicine Press and Springer-Verlag Berlin Heidelberg 2016

\*Supported by the Innovation Fund of Huazhong University of Science and Technology (No. 2013QN235) and the National Natural Science Foundation of China (Nos. 81403257, 81273907, 81102692, 81072493)

Department of Integrated Traditional Chinese and Western Medicine, Union Hospital, Tongji Medical College, Huazhong University of Science and Technology, Wuhan (430022), China  
 Correspondence to: Dr. YANG Yan-ping, Tel: 86-27-85726395, E-mail: [bobo3137@126.com](mailto:bobo3137@126.com)

DOI: <https://doi.org/10.1007/s11655-016-2604-0>

resolution scanning technique, is considered as the most sensitive and accurate method for the study of osteoporosis caused by various conditions and for the evaluation of disease severity. Micro-CT allows 3D analysis of bone density and its microstructure and investigates the structure and function of the bone through assessment of the trabecular structure.<sup>(5-7)</sup>  $\beta$ -Catenin, an important signaling molecule of the Wnt pathway, plays a major role in osteoblast differentiation, proliferation and apoptosis.<sup>(8)</sup> It was reported that oestrogen regulation of  $\beta$ -catenin-dependent transcription might also occur independently of canonical Wnt signaling.<sup>(9-11)</sup> Qing'e Pill (青娥丸, QEP) has been used in Chinese medicine since the Song Dynasty (10th century CE) and is commonly used clinically as an oestrogen agonist for the treatment of osteoporosis,<sup>(12)</sup> particularly in postmenopausal women, but its mechanism of action remains to be elucidated, in particular its link to  $\beta$ -catenin expression.

In the present study, the micro-CT technique was employed to reconstruct and analyse the 3D structure of cancellous bone of the lumbar vertebra and the femur in an ovariectomy-induced osteoporosis mouse model to evaluate the effect of QEP on osteoporosis. Furthermore, the underlying mechanism of the effect of QEP was investigated through the direct assessment of the shape, the structure, and the 3D bone geometry of the trabeculae.

## METHODS

### Drug Preparation

The ingredients of QEP consisting of *Eucommia ulmoides* (960 g), *Fructus Psoraleae* (480 g), *Semen Juglandis* (300 g), and *Allium Sativum* L. (240 g), were washed and placed in a multifunctional extractor. The herbs were immersed in 5-fold their volume of regular water for 2 h followed by boiling for 2 h. After filtering of the boiled decoction, the herbal residues were repeatedly boiled twice 1 h for each time and the resulting boiled decoction was filtered, combined with the first filtrate, and condensed to a thick paste (100%), which was added in 3-fold its volume of 95% ethanol under stirring. After standing for 24 h, the solution was filtered to recover the ethanol fraction, which was concentrated to a decoction of 5 g/mL.<sup>(12)</sup> The dose calculation of QEP and Oestradiol Valerate Tablets (Bu Jia Le, Guangzhou Pharmaceutical Branch of Bayer, China) was in accordance with guidelines correlating

dose equivalents between humans and laboratory animals, based on the ratio of the body surface area.<sup>(13)</sup>

### Animal Grouping, Intervention and Sampling

Ninety-six 8-week-old specific pathogen-free (SPF) C57BL/6 mice, weighing  $21 \pm 2.4$  g, were purchased from the Experimental Animal Center of Huazhong University of Science and Technology, Wuhan, China [batch No. 0237269, certification No. SYXK (Hubei) 2010-0057]. Disinfected food and water were provided under sterile conditions. After 1-month normal feeding, the animals were randomly divided into 4 groups by a random number table consisting of 24 animals each: the sham, ovariectomised osteoporosis model, oestradiol-treated, and QEP-treated groups.

The animals in the model, oestradiol-treated and QEP-treated groups were anaesthetised with an intraperitoneal injection of 1% pentobarbital sodium (30 mg/kg body weight) and maintained in prone position. Ovariectomy was performed via a midline dorsal incision under sterile conditions after which both ovaries were identified adjacent to the inferior pole of the kidneys in the peritoneal cavity, the blood vessels were tied off using No. 4 suture, and both ovaries were removed. The tissue layers were closed and sutured. Starting from post-operative day 5, a pap smear (once per day) was taken from each animal for 5 consecutive days. A successful bilateral ovariectomy was confirmed by a pap smear screening showing the absence of keratosis. Samples exhibiting keratosis were discarded. The animals in the model, oestradiol-treated and QEP-treated groups received 0.5 mL saline, 0.5 mL of a solution containing dissolved Oestradiol Valerate Tablets, and 0.5 mL of QEP solution 1.7 g/kg body weight per day respectively via intragastric gavage from post-operative day 7 onwards.<sup>(13)</sup> Only the adipose tissue surrounding the ovaries, with a weight equivalent to that of both ovaries, was removed in the animals of the sham group and the animals received 0.5 mL saline/day via intragastric gavage from post-operative day 7 onwards.

None of the animals received antibiotics after surgery. Animals were fed under consistent conditions and moving was allowed *ad libitum*. After a 3-month treatment period, the animals were sacrificed using an overdose of anaesthesia and the 3rd lumbar vertebra and the left femur of the animals were dissected immediately. The attached muscle and soft tissue

were removed and the samples were wrapped in saline-soaked gauze for further tests.

### Immunohistochemical Study of $\beta$ -Catenin Expression in Bone Tissue

Four micrometer-thick bone tissue sections were deparaffinised with xylene twice for 10 min followed by rehydration in decreasing concentrations of ethanol ( $1 \times 100\%$ ,  $1 \times 90\%$ , and  $1 \times 80\%$ , respectively) for 10 min/concentration. After a 5-min wash with phosphate-buffered saline (PBS), the samples were incubated in 3% methanol-hydrogen peroxide at room temperature for 15 min to inactivate endogenous peroxidase. Samples were subsequently washed with PBS 3 times for 5 min each, treated with a heated ethylenediaminetetraacetic acid (EDTA) antigen retrieval solution in a microwave oven set at high heat mode for 2.5 min and on defrost mode for 10 min, and were subsequently cooled down for 30 min at room temperature. Samples were washed with PBS 3 times for 5 min each, blocked with 10% goat serum, and incubated in a wet box at room temperature for 30 min followed by incubation with a goat anti-mouse  $\beta$ -catenin antibody in a wet box at room temperature for 30 min. Following a PBS wash 3 times for 5 min each, the samples were incubated with 3,3'-diaminobenzidine and the chromogenic reaction was stopped by washing in tap water. The samples were stained in Mayer's hematoxylin for 20 s and rinsed in tap water. Finally, the slides were dehydrated in a graded ethanol series ( $1 \times 80\%$ ,  $1 \times 90\%$ , and  $1 \times 100\%$ , respectively) for 10 min/concentration, cleared in xylene, and mounted in neutral resin. The immunostaining was assessed by two independent observers. First, the percentage of immunostaining was evaluated, and then, the staining intensity was recorded.

### Micro-CT Imaging

The trabecular microstructure and a 3D image of the 3rd lumbar vertebra and left femur were analysed using the Locus SP Micro-CT System (GE Healthcare, USA, provided by the Hospital of Stomatology, Wuhan University, China). Samples were placed in the sample holder of the scanner and scans were made along the longitudinal axis of the specimen. Consecutive micro-CT images were captured. The image size was set at  $2048 \times 1024$  pixels with a pixel size of  $20 \mu\text{m} \times 20 \mu\text{m}$  and a distance of  $20 \mu\text{m}$  between sections. Scans were made using the following scanning parameters: 60 kV,

400  $\mu\text{A}$ , a  $2^\circ$  rotation step, a  $360^\circ$  rotation angle, an exposure time of 142 s, a voxel size of  $10.34 \mu\text{m}$ , a field of view of  $10.58 \text{ mm} \times 21.17 \text{ mm}$ , and a 30 min scan duration for each specimen. A preliminary scan was made on a reference standard for calibration purposes. Image reconstruction was implemented using the COBRA software with a voxel size of  $0.17 \mu\text{m} \times 5.17 \mu\text{m} \times 10.34 \mu\text{m}$ . The region of interest (ROI) was selected for 3D analysis. Structures with a CT value of  $>1000$  were defined as bone tissue. 3D morphometric parameters were calculated for the selected trabecular ROIs using either direct or indirect measurements. The parameters included (1) the trabecular bone volume fraction (BV/TV), bone volume (BV), and total tissue volume (TV); (2) the trabecular spacing (Tb.Sp); (3) the trabecular thickness (Tb.Th); (4) the trabecular number (Tb.N); (5) the structure model index (SMI); and (6) the bone surface to bone volume ratio (BS/BV).

### Statistical Analysis

Data were presented as mean  $\pm$  standard deviation ( $\bar{x} \pm s$ ). Statistical analyses were performed using the Kruskal-Wallis test or analysis of variance (ANOVA) followed by the Student's *t*-test for multiple comparisons using the SPSS software (version 13.0, SPSS, Inc., Chicago, IL, USA). A *P* value less than 0.05 was considered statistically significant.

## RESULTS

### Survival Outcome

One mouse in the QEP-treated group accidentally died due to anaesthesia while all other mice survived without any incidence of infection.

### $\beta$ -Catenin Expression

$\beta$ -Catenin expression was significantly decreased in bone tissue cells of the model group compared with that of the sham group ( $P < 0.05$ ). In contrast,  $\beta$ -catenin expression in bone tissue cells of the oestradiol-treated and the QEP-treated group was significantly higher than that in that of the ovariectomised osteoporosis model group ( $P < 0.05$ ), but was significantly lower than that in the sham group ( $P < 0.05$ ). No differences in  $\beta$ -catenin expression were observed between bone tissue cells of the oestradiol-treated and QEP-treated groups (Figure 1).

### 3D Micro-CT Imaging of Mice Femur and Lumbar

The parameters of the trabecular bone after 3D

reconstruction demonstrated that the bone density was significantly decreased, bone microarchitecture was severely impaired, trabeculae were thin and less dense, connectivity was reduced, rod-like trabeculae outnumbered plate-like structures, and larger intertrabecular spaces were present in animals of the model group (Figure 2). Furthermore, BV/TV, Tb.N, and Tb.Th were significantly decreased and SMI, Tb.Sp, and BS/BV were significantly increased compared with those of the sham group in both femur and lumbar ( $P<0.05$ ), indicating the successful establishment of the experiment model (Table 1).

Compared with the trabecular bone structure of the model group, that of both the oestradiol-treated and the QEP-treated groups were significantly improved. This was shown by an increased number

of trabeculae parallel-arranged in the same direction, decreased porosity, and a significantly increased BV/TV, Tb.N, and Tb.Th compared with those of the ovariectomised osteoporosis model group ( $P<0.05$ ). The SMI, Tb.Sp, and BS/BV, however, were significantly decreased compared with those of the ovariectomised osteoporosis model group in both femur and lumbar of mice ( $P<0.05$ , Table 1).

No significant differences were found in the micro-CT imaging parameters of the femur between animals of the oestradiol-treated and the QEP-treated groups. The only difference was found in the Tb.Th of the lumbar vertebra, which was significantly higher in animals of the oestradiol-treated group than that of the QEP-treated group ( $P<0.05$ , Table 1).

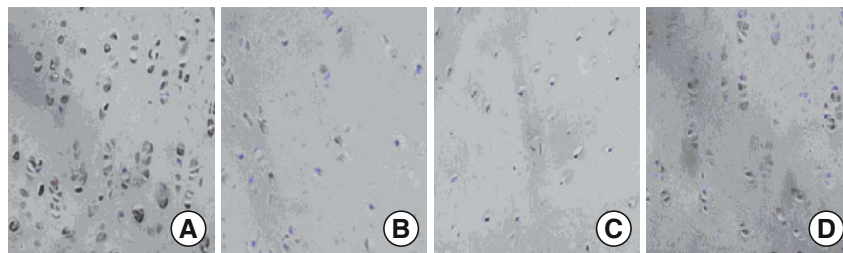


**Figure 1. Expression of  $\beta$ -Catenin of Mice Lumbar Tissue in Each Group (IHC,  $\times 400$ )**

Notes: A: sham group, B: model group, C: oestradiol-treated group, D: QEP-treated group

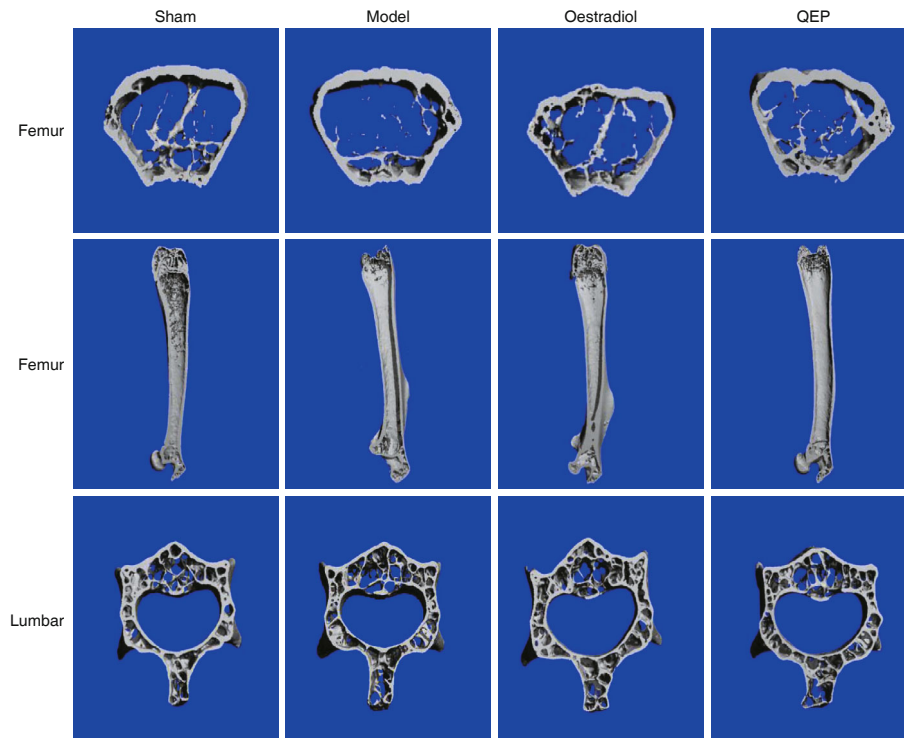


**Figure 2. Micro-CT of Left Femur and Lumbar of Mice in Four Groups**

**Table 1. Comparison of Micro-CT Parameters of Femur and Lumbar in Mice among Four Groups ( $\bar{x} \pm s$ )**

Parameters	Sham group (n=24)	Model group (n=24)	Oestradiol-treated group (n=24)	QEP-treated group (n=23)
<b>Femur</b>				
BV/TV	0.311 ± 0.013	0.217 ± 0.062*	0.282 ± 0.008 <sup>△</sup>	0.275 ± 0.021 <sup>△</sup>
SMI	0.176 ± 0.112	1.359 ± 0.147*	0.698 ± 0.175* <sup>△</sup>	0.674 ± 0.392* <sup>△</sup>
Tb.N (mm <sup>-1</sup> )	3.060 ± 0.168	2.259 ± 0.165*	2.756 ± 0.131* <sup>△</sup>	2.705 ± 0.145* <sup>△</sup>
Tb.Th (mm)	0.129 ± 0.005	0.105 ± 0.003*	0.117 ± 0.005* <sup>△</sup>	0.113 ± 0.003* <sup>△</sup>
Tb.Sp (mm)	0.339 ± 0.015	0.454 ± 0.038*	0.372 ± 0.014* <sup>△</sup>	0.383 ± 0.023* <sup>△</sup>
BS/BV (mm <sup>-1</sup> )	16.429 ± 0.901	21.585 ± 1.014*	18.865 ± 0.718* <sup>△</sup>	19.256 ± 0.882* <sup>△</sup>
<b>Lumbar</b>				
BV/TV	0.275 ± 0.005	0.199 ± 0.001*	0.237 ± 0.022* <sup>△</sup>	0.240 ± 0.016* <sup>△</sup>
SMI	0.064 ± 0.042	0.501 ± 0.124*	0.233 ± 0.076* <sup>△</sup>	0.232 ± 0.066* <sup>△</sup>
Tb.N (mm <sup>-1</sup> )	4.126 ± 0.286	2.636 ± 0.084*	3.215 ± 0.406* <sup>△</sup>	3.115 ± 0.290* <sup>△</sup>
Tb.Th (mm)	0.076 ± 0.005	0.060 ± 0.002*	0.068 ± 0.005* <sup>△</sup>	0.063 ± 0.004* <sup>△▲</sup>
Tb.Sp (mm)	0.268 ± 0.017	0.472 ± 0.008*	0.401 ± 0.036* <sup>△</sup>	0.418 ± 0.043* <sup>△</sup>
BS/BV (mm <sup>-1</sup> )	25.065 ± 1.937	33.036 ± 0.590*	29.363 ± 1.640* <sup>△</sup>	29.228 ± 1.945* <sup>△</sup>

Notes: \* $P < 0.05$  vs. sham group; <sup>△</sup> $P < 0.05$  vs. model group; <sup>▲</sup> $P < 0.05$  vs. oestradiol-treated group

## DISCUSSION

Pathological changes of osteoporosis include qualitative and quantitative alterations. Quantitative alterations are characterized by a decrease in BMD while qualitative alterations are manifested by changes in the growth condition of the trabecular bone, bone mineralization, area of bone accumulation, and micro-injury, resulting in regional morphological changes, such as a decrease in the volume of both cortical and trabecular bones and a disruption and thinning of trabeculae. Increasing evidence has demonstrated that BMD measurement is not a comprehensive method for the evaluation of changes in the mechanical properties of osteoporotic bones.<sup>(15,16)</sup> On the one hand, slight changes (5%–8%) in BMD will result in about 60% alterations in the mechanical properties of bone in response to mechanical loads; on the other hand, DEXA is a widely used modality for the measurement of bone mineral content. However, this two-dimensional scanning technique cannot differentiate between the various soft tissue compositions present within the X-ray beam, including red and yellow bone marrow and muscle and adipose tissue, which are then inevitably considered as mineral content, leading to inaccuracy (an increase or decrease) in measuring BMD. An accuracy error of 20% was reported for DEXA and even an accuracy error of 30% was reached when measuring minerals in bones of low mass (osteoporotic bone or callus tissue).<sup>(17,18)</sup> Several animal experiments and clinical studies have shown that by just increasing

BMD, bone strength is not increased accordingly; on the contrary, a decrease in strength has been observed occasionally.<sup>(19,20)</sup>

The emergence of the micro-CT technique has deepened the understanding of the microarchitecture of osteoporosis.<sup>(21,22)</sup> Micro-CT scanning can differentiate between cortical and cancellous bone while acquiring intuitive high-resolution 3D images.<sup>(23)</sup> In addition, this technique allows for quantitative analysis, which provides multiple parameters, enabling multi-aspect comparisons and providing tremendous convenience for the study of small animals, especially of mice and of several mouse models of disease.<sup>(24)</sup> Of the microstructural parameters measured by the micro-CT technique, BV/TV, which represents the percentage of trabecular bone volume to total volume of bone tissue, is one of the most important parameters for depicting the microstructure of cancellous bone in that it reflects the volume of bone tissue in cancellous bone. Furthermore, Tb.Th represents the average thickness of trabecular bone; Tb.N is defined as the number of intersections between bone tissue and non-bone components within a defined length of specimen; and Tb.Sp provides the average width of the trabecular bone marrow. Altogether, these parameters indicate geometry features of trabecular bone. SMI is an additional variable for depicting the 3D geometry of subjects, representing the structural properties of trabecular bone, and is used for depicting the surface curvature of subjects. SMI is an index evaluating

whether trabecular bone is rod-like or plate-like, thereby reflecting the ratio between plate-like and rod-like structures. For an ideal plate-like and rod-like structure, the SMI has a value of 0 and 3, respectively. Under normal physiological conditions, cancellous bone is composed of a mixture of both plate-like and rod-like structures, which has a SMI value within a 0–3 range. In osteoporosis, plate-like trabeculae are converted to a rod-like structure, increasing the SMI value.

In this study, we discovered that the number of trabeculae was decreased, the inter-trabecular space was increased, and the connectivity of the trabecular bone structure was disrupted in ovariectomised mice. The SMI values of ovariectomised animals increased compared with those of the animals in the sham group, which is consistent with previously reported results.<sup>(25)</sup> The increase in the SMI value may have been the result of enhanced osteoclastic resorption at the bone surface caused by decreased oestrogen. Osteoclastic resorption becomes larger than osteoblastic bone formation, resulting in the gradual expansion of the resorption area, which develops into a condition where plate-like trabeculae are gradually converted into a rod-like structure. In addition, the BV/TV, Tb.N, and Tb.Th of the animals in the oestradiol-treated group were significantly increased compared with those of the animals of the ovariectomised osteoporosis model group ( $P < 0.05$ ); the Tb.Sp and BS/BV, however, were significantly decreased compared with those of the animals of the ovariectomised osteoporosis model group ( $P < 0.05$ ). This was partially because the post-ovariectomy decline of oestrogen results in a significant alteration of the microstructure of cancellous bone, characterized by the conversion of plate-like trabeculae to a rod-like structure, increased trabecular separation, and a reduced number of trabecular bones. This reduces the mechanical properties of the bone; the intervention with oestrogen is able to partially restore the microstructure of cancellous bone, thereby improving its mechanical properties.

In the current study, no significant differences as were observed in the micro-CT imaging parameters of the lumbar vertebra were found in those of the femur between animals of the oestradiol-treated and the QEP-treated group. Among the four ingredients, the principal herb parts *Eucommia ulmoides* and *Fructus Psoraleae* have been reported to contain flavonoids,

lignans, and coumarins, which are oestrogen-like compounds.<sup>(26,27)</sup> QEP has been shown to treat postmenopausal symptoms through its action as an oestrogen agonist.<sup>(12)</sup> In the present study, QEP seems to be as effective as an anti-osteoporosis drug as oestradiol Valerate Tablets.

Wnt/ $\beta$ -catenin signalling has currently been recognized as an important regulator of bone mass and bone cell differentiation. It cross-talks with other signaling pathways, including oestrogen receptor signaling.<sup>(28)</sup> Both the Wnt/ $\beta$ -catenin and oestrogen receptor signaling pathways play an important role in bone remodeling, particularly in menopausal women.<sup>(29)</sup> The main purpose of this study was to investigate the mechanisms by which a phytoestrogen function from QEP prevents bone loss in oestrogen deficiency, with a specific emphasis on the activation of  $\beta$ -catenin expression. The present study shows that  $\beta$ -catenin expression was not different between the oestradiol-treated and the QEP-treated group, but that the expression was significantly higher in both groups than that of the ovariectomised osteoporosis model group. Our preliminary studies showed a significant positive correlation between the serum levels of  $\beta$ -catenin and those of osteoprotegerin, a negative correlation between sclerostin, and the ratio of receptor activator of nuclear factor kappa B ligand (RANKL)/osteoprotegerin (OPG),<sup>(30)</sup> which suggest that  $\beta$ -catenin signaling contributed to bone growth and bone remodeling. These findings are consistent with our micro-CT imaging results. Taken together, our results strongly suggest that QEP strengthens the quality and quantity of bone through the activation of  $\beta$ -catenin expression, which is mediated through a non-genomic estrogenic action.

Our previous studies showed that QEP had an effect on the special sequence of  $\beta$  collagen in blood markers of bone metabolism, such as  $\beta$ -crossLaps, N-terminal osteocalcin, total procollagen type I N-terminal propeptide, and vitamin D receptor mRNA expression in postmenopausal osteoporosis, thereby effectively controlling osteoporosis.<sup>(30,31)</sup> Furthermore, we also showed a similar drug efficacy between QEP and active vitamin D<sub>3</sub>, because both were able to increase VDR mRNA expression in the body, reduced bone resorption, and increased the quality and the quantity of bones.<sup>(29)</sup> These results suggest that QEP, prepared using an ancient recipe, has

comparable efficacy in the prevention and treatment of postmenopausal osteoporosis as a sufficient supplement of active vitamin D<sub>3</sub> has. In other studies, we demonstrated that a low level of  $\beta$ -catenin is likely to be associated with the onset of postmenopausal osteoporosis.<sup>(31-34)</sup> In our current work, we further studied the mechanism underlying the treatment of osteoporosis by using the QEP because it shows that the interaction between the Wnt/ $\beta$ -catenin and the RANKL/RANK/OPG signaling pathways might play an important role in the pathogenesis of postmenopausal osteoporosis.<sup>(12,31)</sup> Indeed, the effect of QEP on osteoporosis might be achieved by elevating the bone mass through the improved expression of  $\beta$ -catenin, as shown by the significant improvement of the trabecular microstructure, the increase in the number of trabecular bone structures parallel-arranged in the same direction, and the reduction of porosity. However, further studies are required to elucidate this mechanism in more detail.

### Conflict of Interests

The authors declare that they have no conflict of interest.

### Author Contributions

Shuai B, Yang YP, and Shen L conceived and designed the experiments; Zhu R, Xu XJ, Ma C, and Lu L performed the experiments. Shuai B, Yang YP, Shen L, and Zhu R analyzed the data; Shuai B and Yang YP contributed to reagents/materials/analysis tools; Shuai B wrote the manuscript. All authors critically read and approved the final manuscript.

### Acknowledgements

The authors would like to thank XIA Xue for his expertise and assistance in performing the blood collection, and WANG Quan-shen for his technical assistance, both from Union Hospital of Tongji Medical College, Huazhong University of Science and Technology.

## REFERENCES

- Poole KE, Treece GM, Gee AH, Brown JP, McClung MR, Wang A, et al. Denosumab rapidly increases cortical bone in key locations of the femur: a 3D bone mapping study in women with osteoporosis. *J Bone Miner Res* 2015;30:46-54.
- Klodowski K, Kaminski J, Nowicka K, Tarasiuk J, Wroński S, Świątek M, et al. Micro-imaging of implanted scaffolds using combined MRI and micro-CT. *Comput Med Imag Graph* 2014;38:458-468.
- Knapp KM, Welsman JR, Hopkins SJ, Shallcross A, Fogelman I, Blake GM. Obesity increases precision errors in total body dual-energy X-ray absorptiometry measurements. *J Clin Densitom* 2015;18:209-216.
- Ontario HQ. Utilization of DXA bone mineral densitometry in Ontario: an evidence-based analysis. *Ont Health Technol Assess Ser* 2006;6:1-180.
- Wurnig MC, Calcagni M, Kenkel D, Vich M, Weiger M, Andreisek G, et al. Characterization of trabecular bone density with ultra-short echo-time MRI at 1.5, 3.0 and 7.0 T comparison with micro-computed tomography. *NMR Biomed* 2014;27:1159-1166.
- Effendy NM, Khamis MF, Soelaiman IN, Shuid AN. The effects of *Labisia pumila* on postmenopausal osteoporotic rat model: dose and time-dependent micro-CT analysis. *J Xray Sci Technol* 2014;22:503-518.
- Ramli R, Khamis MF, Shuid AN. Bone micro-CT assessments in an orchidectomised rat model supplemented with *Eurycoma longifolia*. *Evid Based Complement Alternat Med* 2012;50:1858.
- Holmen SL, Zylstra CR, Mukherjee A, Sigler RE, Faugere MC, Bouxsein ML, et al. Essential role of beta-catenin in postnatal bone acquisition. *J Biol Chem* 2005;280:21162-21168.
- Chen Q, Zhuang Q, Mao W, Xu XM, Wang LH, Wang HB. Inhibitory effect of cryptotanshinone on angiogenesis and Wnt/ $\beta$ -catenin signaling pathway in human umbilical vein endothelial cells. *Chin J Integr Med* 2014;20(10):743-750
- Xu YX, Wu CL, Wu Y, Tong PJ, Jin HT, Yu NZ, et al. Epimedium-derived flavonoids modulate the balance between osteogenic differentiation and adipogenic differentiation in bone marrow stromal cells of ovariectomized rats via Wnt/ $\beta$ -catenin signal pathway activation. *Chin J Integr Med* 2012;18:909-917.
- Li FL, Deng H, Wang HW, Xu R, Chen J, Wang YF, et al. Effects of external application of Chinese medicine on diabetic ulcers and the expressions of  $\beta$ -catenin, c-myc and K6. *Chin J Integr Med* 2011;17:261-266.
- Xu Y, Zhang ZJ, Geng F, Su SB, White KN, Bligh SW, et al. Treatment with Qing'e, a kidney-invigorating Chinese herbal formula, antagonizes the estrogen decline in ovariectomized mice. *Rejuvenation Res* 2010;13:479-488.
- Contrera JF, Matthews EJ, Kruhlak NL, Benz RD. Estimating the safe starting dose in phase I clinical trials and no observed effect level based on QSAR modeling of the human maximum recommended daily dose. *Regul Toxicol Pharmacol* 2004;40:185-206.
- Khajuria DK, Razdan R, Mahapatra DR. Zoledronic acid in combination with alfacalcidol has additive effects on trabecular microarchitecture and mechanical properties in osteopenic ovariectomized rats. *J Orthop Sci* 2014;19:646-656.
- Jiang Y, Zhao J, Rosen C, Geusens P, Genant HK. Perspectives on bone mechanical properties and adaptive

- response to mechanical challenge. *J Clin Densitom* 1999;2:423-433.
16. Hahn M, Vogel M, Pompesius-Kempa M, Delling G. Trabecular bone pattern factor—a new parameter for simple quantification of bone microarchitecture. *Bone* 1992;13:327-330.
  17. Warden SJ, Hurst JA, Sanders MS, Turner CH, Burr DB, Li J. Bone adaptation to a mechanical loading program significantly increases skeletal fatigue resistance. *J Bone Miner Res* 2005;20:809-816.
  18. Bolotin HH, Sievanen H. Inaccuracies inherent in dual-energy X-ray absorptiometry *in vivo* bone mineral density can seriously mislead diagnostic/prognostic interpretations of patient-specific bone fragility. *J Bone Miner Res* 2001;16:799-805.
  19. Legrand E, Chappard D, Pascaretti C, Duquenne M, Krebs S, Rohmer V, et al. Trabecular bone microarchitecture, bone mineral density, and vertebral fractures in male osteoporosis. *J Bone Miner Res* 2000;15:13-19.
  20. Verborgt O, Gibson GJ, Schaffler MB. Loss of osteocyte integrity in association with microdamage and bone remodeling after fatigue *in vivo*. *J Bone Miner Res* 2000;15:60-67.
  21. Park YS, Kim S, Oh SH, Park HJ, Lee S, Kim TI, et al. Comparison of alveolar ridge preservation methods using three-dimensional micro-computed tomographic analysis and two-dimensional histometric evaluation. *Imaging Sci Dent* 2014;44:143-148.
  22. Neves AA, Jaecques S, Van Ende A, Cardoso MV, Coutinho E, Lührs AK, et al. 3D-microleakage assessment of adhesive interfaces: exploratory findings by  $\mu$ CT. *Dent Mater* 2014;30:799-807.
  23. Laib A, Barou O, Vico L, Lafage-Proust MH, Alexandre C, Rugseger P. 3D micro-computed tomography of trabecular and cortical bone architecture with application to a rat model of immobilisation osteoporosis. *Med Biol Eng Comput* 2000;38:326-332.
  24. Du LY, Umoh J, Nikolov HN, Pollmann SI, Lee TY, Holdsworth DW. A quality assurance phantom for the performance evaluation of volumetric micro-CT systems. *Physics Med Biol* 2007;52:7087-7108.
  25. Kinney JH, Haupt DL, Balooch M, Ladd AJ, Ryaby JT, Lane NE. Three-dimensional morphometry of the L6 vertebra in the ovariectomized rat model of osteoporosis: biomechanical implications. *J Bone Miner Res* 2000;15:1981-1991.
  26. Sirtori CR, Arnoldi A, Johnson SK. Phytoestrogens: end of a tale? *Ann Med* 2005;37:423-438.
  27. Moon YJ, Wang X, Morris ME. Dietary flavonoids: effects on xenobiotic and carcinogen metabolism. *Toxicol In Vitro* 2006;20:187-210.
  28. Kouzmenko AP, Takeyama K, Ito S, Furutani T, Sawatsubashi S, Maki A, et al. Wnt/ $\beta$ -catenin and estrogen signaling converge *in vivo*. *J Biol Chem* 2004;279:40255-40258.
  29. Liedert A, Wagner L, Seefried L, Ebert R, Jakob F, Ignatius A. Estrogen receptor and Wnt signaling interact to regulate early gene expression in response to mechanical strain in osteoblastic cells. *Biochem Biophys Res Commun* 2010;394:755-759.
  30. Shuai B, Yang YP, Shen L, Ke H. Effects of Qing'e Formula on the expression of bone metabolic markers and VDR mRNA in postmenopausal osteoporosis patients. *Chin Med* 2014;5:145-152.
  31. Xu XJ, Shen L, Yang YP, Zhu R, Shuai B, Li CG, et al. Serum beta-catenin Levels associated with the ratio of RANKL/OPG in patients with postmenopausal osteoporosis. *Int J Endocrinol* 2013;2013:534352.
  32. Xu XJ, Shen L, Yang YP, Lu FR, Zhu R, Shuai B, et al. Serum sclerostin levels associated with lumbar spine bone mineral density and bone turnover markers in patients with postmenopausal osteoporosis. *Chin Med J* 2013;126:2480-2484.
  33. Shuai B, Shen L, Yang YP, Xie J, Shou ZX, Wei B. Low plasma adiponectin as a potential biomarker for osteonecrosis of the femoral head. *J Rheumatol* 2010;37:2151-2155.
  34. Yang YP, Shuai B, Shen L, Xu XJ, Ma C, Lv L. Effect of Qing'e Formula on circulating sclerostin levels in patients with postmenopausal osteoporosis. *J Huazhong Univ Sci Technol (Med Sci)* 2015;35:645-648.

(Received August 26, 2014; First Online October 24, 2016)  
 Edited by YUAN Lin